

# Appendix A

The peak magnitude of a second-order transfer function is of importance in the scaling of the internal node voltage in a biquad realized using several active devices such as opamps or operational transconductance amplifiers. Closed-form solutions in terms of the coefficients of the numerator and denominator of the second-order transfer function will be beneficial in computer-aided design programs. Table A.1 gives these in the case of both analog and digital transfer functions.

The second-order digital transfer function considered is

$$H(z) = \frac{pz^2 - qz + r}{z^2 - uz + v} \tag{A.1}$$

Using bilinear transformation and considering without loss of generality  $T = 2$  s, we have

$$H(s) = \frac{\left(\frac{p+q+r}{1+u+v}\right)s^2 + s\frac{2(p-r)}{1+u+v} + \frac{p-q+r}{1+u+v}}{s^2 + s\frac{2(1-v)}{1+u+v} + \frac{1-u+v}{1+u+v}} \tag{A.2}$$

or

$$H(s) = \frac{as^2 + bs + c}{s^2 + ds + e} \tag{A.3}$$

The peak or valley of (A.3) can be found by equating the squared magnitude  $|H(j\omega)|^2$  with  $K^2$ . The resulting quadratic equation in  $\omega^2$  will have equal roots in the case where the solution corresponds to a peak or valley. This yields the relationship:

$$K^4(d^4 - 4e d^2) + K^2(4b^2 e - 8ace - 2b^2 d^2 + 4ac d^2 + 4c^2 + 4a^2 e^2) + (b^4 - 4b^2 ac) = 0 \tag{A.4}$$

**Table A.1** (Adapted from [A.1] © IEEE 1983)

	Type of transfer function	Magnitude of the peak
1	Band-pass (bilinear) $a = c = 0$	$\frac{p-r}{1-v}$
2	Low-pass (bilinear) $a = b = 0$	$\frac{(p-q+r)(1+u+v)}{2(1-v)\sqrt{4v-u^2}}$
3	High-pass (bilinear) $b = c = 0$	$\frac{(p+q+r)(1-u+v)}{2(1-v)\sqrt{4v-u^2}}$
4	Notch $b = 0$	$\frac{2\sqrt{ac d^2 + c^2 + a^2} e^2 - 2ace}{d\sqrt{4e-d^2}}$
5	All-pass $u = \frac{q}{r}$ and $v = \frac{p}{r}$	$r$
6	General biquadratic function	$\frac{-y + \sqrt{y^2 - 4xz}}{2x}$

The quadratic equation in  $K^2$  can be solved to obtain the peak and/or valley values of  $K$ . For special cases such as a band-pass transfer function, for example,  $a = c = 0$ , simple cases, the expression will be much simpler. Since the design of digital filters based on a bilinear  $s \rightarrow z$  transformation starts with an analog prototype transfer function, (A.4) can be used directly to obtain  $K$  in terms of  $a$ ,  $b$ ,  $c$ ,  $d$ , and  $e$ . In other cases, formulae in Table A.1 will be useful. Note that we have defined

$$x = d^4 - 4e d^2, y = 4b^2 e - 8ace - 2b^2 d^2 + 4ac d^2 + 4c^2 + 4a^2 e^2, z = b^4 - 4b^2 ac$$

in entry 6 in Table A.1.

Note also that from (A.1) directly, the peak or valley value can be found without using bilinear transformation. In this approach,  $z = e^{j\omega T}$  is substituted to obtain first the relationship

$$K^2 = \frac{a_o \cos^2 \omega T - b_o \cos \omega T + c_o}{\cos^2 \omega T - d_o \cos \omega T + e_o} \quad (\text{A.5})$$

where  $a_o = \frac{pr}{v}$ ,  $b_o = \frac{(p+r)q}{2v}$ ,  $c_o = \frac{(p-r)^2 + q^2}{4v}$ ,  $d_o = \frac{(1+v)u}{2v}$ ,  $e_o = \frac{(1-v)^2 + u^2}{4v}$ .

From (A.5), the peak or valley can be found by following a similar approach as described in the case of (A.3), from the equation

$$K^4 (d_o^2 - 4e_o) + K^2 (4c_o + 4a_o e_o - 2b_o d_o) + (b_o^2 - 4a_o c_o) = 0 \quad (\text{A.6})$$

Laakso has pointed out that in both approaches described above,  $K$  is real. In the case where  $K$  is not real, the value of the transfer function at dc and infinite frequencies needs to be found and the higher among them is the maximum

magnitude. These are from (A.5) (at  $\cos(\omega T) = 1$  and  $\cos(\omega T) = -1$ ), respectively,

$$K^2 = \frac{a_o - b_o + c_o}{1 - d_o + e_o} \quad \text{and} \quad K^2 = \frac{a_o + b_o + c_o}{1 + d_o + e_o}$$

## References

- [A.1] Ananda Mohan, P.V., Ramachandran, V., Swamy, M.N.S.: Formulas for dynamic range evaluation of second-order discrete-time filters. *IEEE Trans. Circuits Syst.* **CAS-30**, 321 (1983)
- [A.2] Ananda Mohan, P.V., Surajit Sen.: Design of tunable multiple input notch filters. *Proc. IEEE* **66**, 352–354 (1978)
- [A.3] Bomar, B.W., Joseph, R.D.: Calculation of L norms for scaling second-order state-space digital filter sections. *IEEE Trans. Circuits Syst.* **CAS-34**, 983–984 (1987)
- [A.4] Ananda Mohan, P.V.: Comments on “Calculation of L norms for scaling second-order state-space digital filter sections.” *IEEE Trans. Circuits Syst.* **CAS-36**, 310–311 (1989)
- [A.5] Laakso, T.I.: Comments on “Calculation of L norms for scaling second-order state-space digital filter sections.” *IEEE Trans. Circuits Syst. II Analog Digit. Signal Process.* **39**, 256 (1992)

# Appendix B

The realized transfer function is affected by the nonideal passive and active components. The variation in the transfer function due to variations in pole-frequency and pole-Q can first be evaluated. These yield topology-independent expressions or curves. The variation in pole-frequency and pole-Q due to the active and passive components in the chosen topology is topology-dependent and can be estimated easily. Substituting the latter in the former expressions gives the total variation in the transfer function. Considering  $H(s)$  as the desired biquadratic transfer function

$$H(s) = \frac{1}{D(s)} = \frac{1}{s^2 + s\frac{\omega_p}{Q_p} + \omega_p^2} \tag{B.1}$$

we can obtain

$$S_{\omega_p}^{|H(j\omega)|} = - \left( \frac{2(1 - \gamma^2) + \frac{\gamma^2}{Q_p^2}}{(1 - \gamma^2)^2 + \frac{\gamma^2}{Q_p^2}} \right) \tag{B.2}$$

and

$$S_{Q_p}^{|H(j\omega)|} = \left( \frac{\frac{\gamma^2}{Q_p^2}}{(1 - \gamma^2)^2 + \frac{\gamma^2}{Q_p^2}} \right) \tag{B.3}$$

where  $\gamma = \frac{\omega}{\omega_p}$ . It can be seen from (B.2) and (B.3) that both sensitivities are functions of  $\gamma$  and hence universal curves as functions of  $\gamma$  are of interest. These are presented in Fig. B.1a, b [B.1]. It may be noted that  $S_{\omega_p}^{|H(j\omega)|}$  reaches a maximum of about  $Q_p$  at the 3-dB frequencies  $\gamma = 1 \pm \frac{1}{2Q_p}$  whereas the maximum value of  $S_{Q_p}^{|H(j\omega)|}$  is unity. The ratio of  $S_{\omega_p}^{|H(j\omega)|}$  to  $S_{Q_p}^{|H(j\omega)|}$  is

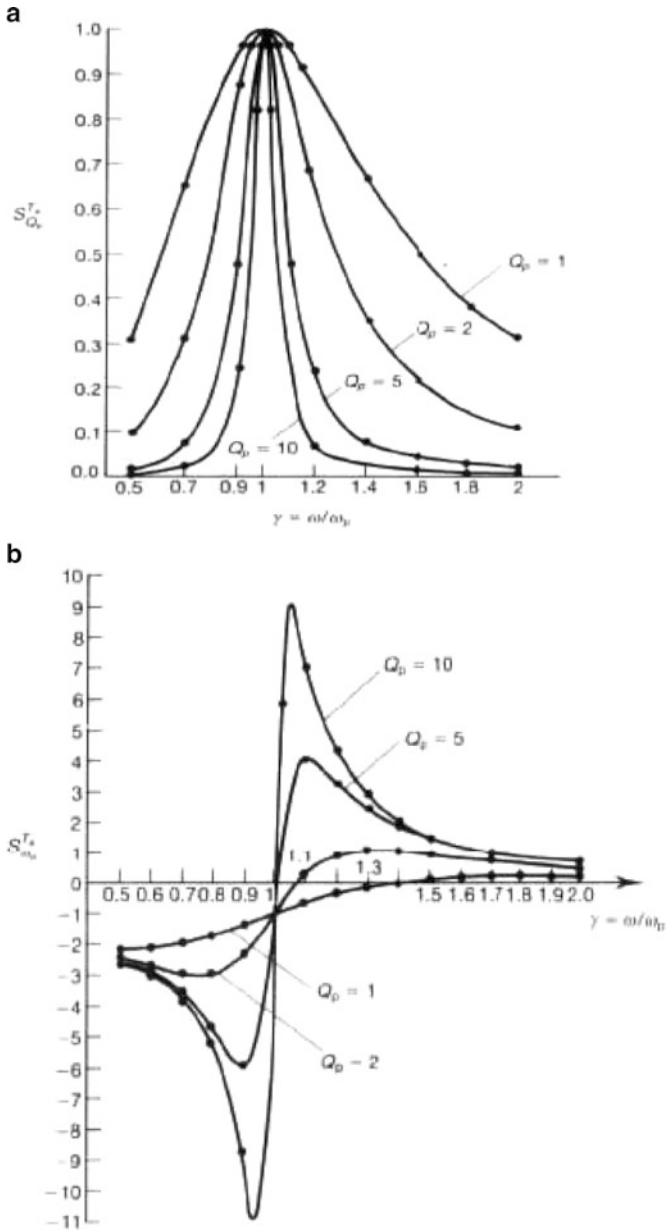


**Fig. B.1** Universal curves showing sensitivity of transfer function to pole-frequency (a) and pole-Q (b) with pole-Q as a parameter (Adapted from [B.1] © IEEE 1973)

$$\frac{S_{\omega_p}^{|H(j\omega)|}}{S_{Q_p}^{|H(j\omega)|}} = - \left( 1 + 2Q_p^2 \left( \frac{1}{\gamma^2} - 1 \right) \right) \quad (\text{B.4})$$

At the 3-dB frequencies, this ratio is  $2Q_p$ . This is an important result showing that the magnitude of sensitivities to pole-frequency must be kept less than  $2Q_p$  times the magnitude of sensitivities to pole-Q.

It can next be observed that the percentage variation in the transfer function can be expressed as

$$\frac{\Delta|H|}{|H|} = S_{\omega_p}^{|H|} \cdot \frac{\Delta\omega_p}{\omega_p} + S_{Q_p}^{|H|} \cdot \frac{\Delta Q_p}{Q_p} \quad (\text{B.5})$$

We next note that

$$\frac{\Delta\omega_p}{\omega_p} = \sum_{i=1}^k S_{C_i}^{\omega_p} \cdot \frac{\Delta C_i}{C_i} + \sum_{i=1}^l S_{R_i}^{\omega_p} \cdot \frac{\Delta R_i}{R_i} \quad (\text{B.6})$$

considering that the filter needs  $k$  capacitors and  $l$  resistors. Note that the active devices also need to be included in the above expressions since we have earlier described the evaluation of pole-Q and pole-frequency sensitivities to opamp finite gain and finite bandwidth.

## Reference

- [B.1] Hilberman, D.: An approach to the sensitivity and statistical variability of biquadratic filters. IEEE Trans. Theory **CT-20**, 382–390 (1973)

# Index

## A

- Active filters using amplifier pole
  - effect of bandwidth on active RC, 81
  - using one capacitor, 76–81
  - using resistors differentiator, 76, 77
- Active- $G_m$ -RC filters, 81, 496
- Active RC filters
  - active compensation of
    - using composite amplifiers, 34, 35
    - using NIC, 20, 21
  - distortion in, 118, 122–126
  - effect of opamp bandwidth on, 6
  - noise analysis of, 112–122
  - passive compensation of, 26, 34
  - using a single fully differential amplifier, 53–55
- Active RC filters for wireless applications
  - ADSL, 462–465
  - Bluetooth, 443, 444, 446, 450
  - PDC, 456, 460
  - software radio, 465
  - UWB, 447, 448
  - WCDMA, 456
  - WLAN/UMTS receivers, 450
  - Zigbee, 443, 446
- Active RC ladder filters based on component simulation, 5, 89–91, 198–201
- Active R filters, 6
- All-pass filters, first order
  - current mode, 153, 235, 236
  - SC, 258
  - using opamps, 30, 126
  - using OTAs, 152, 153, 189–197, 236
- Alternating divide and conquer technique, 471

- Analysis of SC filters
  - SPICE based, 371–373
  - using Laker's Z-domain equivalents, 254–257
- Analytical synthesis technique, 220

## B

- Bandpass sigma-delta modulators, 319, 411–424
- Biased-inverting opamp configuration, 361–365
- Bilinear SC integrators, 283, 316, 317

## C

- CBSC. *See* Comparator based SC circuits (CBSC)
- Charge injection in SC filters, 326, 348, 349, 353, 354, 381–382
- Clock boosting, 355
- Clock feedthrough in SC filters, 268, 307, 311, 313, 325, 355, 387
- Comparator based SC circuits (CBSC), 578–583
- Complementary transformation, 424
- Complex filters, 445, 501, 510, 511, 514, 573
- Composite amplifier, 16, 36
- Correlated Double-sampling, 366
- CT sigma-delta modulators, 383, 590
- Current conveyor, 2, 10, 134, 137, 139, 141, 532, 536, 602
- Current feedback operational amplifier, 10
- Current input current output filters, 129, 134, 152, 518
- Current-mode filter derived from ladder filters, 209–216

**D**

- Deliyannis bandpass filter, 42
- Distortion in
  - active RC filters, 118, 122–126
  - cancellation technique in OTA-C filters, 530, 533
  - OTA-C filters, 235, 237–239
  - SC filters, 346–349
- Dynamic biasing, 456, 471
- Dynamic impedance scaling, 465, 471, 473

**E**

- Evaluation of CT filters, 599–600

**F**

- Field programmable analog array, 556, 560
- Figure of merit (FOM), 123, 423, 590, 599
- FIR filters, 309, 331–337
- Fleischer–Laker biquad
  - E-type, 275
  - F-type, 267, 275, 283
- FLF. *See* Follow-the-leader feedback (FLF)
- Foldover noise, 8, 367, 368, 371
- Follow-the-leader feedback (FLF), 106–111
- FOM. *See* Figure of merit (FOM)
- Four terminal floating nullor (FTFN), 140
- Frequency dependent negative resistance (FDNR), 91–93, 199, 201, 466, 468, 469
  - using Active RC technique, 466–478
  - using OTA-C technique, 198, 199
- Friend's active RC biquad
  - Friend's low-pass filter, 137
  - Steffen all-pass SAB, 130

**G**

- Gain sensitivity product (GSP), 45
- GIC based biquads, 55–58
- $G_m$ -assisted filters, 476
- $G_m$ -C filters, 1, 8, 148, 447, 448, 478–578
- $G_m$ -Opamp integrator, 149
- GSP, Gain sensitivity product (GSP)

**I**

- IFLF. *See* Inverse follow-the-leader feedback (IFLF)
- Inductance realization
  - floating, 91, 92
  - grounded, 89, 92

- using opamp and RC, 91, 92
- using OTA and C, 171, 178, 180, 182, 184, 291, 481
- using SC, 92, 290, 429
- Inductance simulation using amplifier pole
- Integrated resistors and capacitors, 439–440
- Integrators
  - active RC, 9, 252
  - Akerberg–Mossberg integrator, 22, 24, 96
  - Deboo's integrator, 24
  - differential integrator, 27, 73, 149, 290, 382
  - OTA-C, 148–149
  - Q-factor of, 24
  - SC, 253, 255, 278, 331, 337–346, 351, 359, 374, 375, 583
- Inverse follow-the-leader feedback (IFLF), 107, 110, 111

**K**

- KHN biquad
  - active RC, 172, 233, 234
  - current-mode, 59–63, 68–74, 234

**L**

- Ladder filters based on
  - component simulation, 89–91, 287–298
  - operational simulation, 89, 93–100, 287–298
- LC filters for UWB receivers
  - linear transformation type OTA-C filters, 202–208
  - lossless discrete integration (LDI), 257
- Lossy inductance simulation, 47
- Low-pass filters
  - active RC, 27–41
  - $G_m$ -C, 539, 543
  - SC, 291–296, 307, 357, 359
- Low-voltage design techniques, 349–365

**M**

- Minimum sensitivity feedback (MSF), 107, 110–111
- MOSFET\_C technique, 505, 510
- MSF. *See* Minimum sensitivity feedback (MSF)
- Multi-loop feedback type active filters
  - follow-the-leader feedback (FLF), 106–111
  - inverse follow-the-leader feedback (IFLF), 107, 110, 111



- minimum sensitivity feedback (MSF), 110–111
  - primary resonator block, 108–109
  - shifted companion form (SCF), 109–110
- Multiple-feedback filters
  - active RC, 42–55, 69, 72, 113, 131
  - OTA-C, 216–219
  - SC,
- Multiplexed SC biquads, 270, 272
- N**
- Nauta's transconductor, 568, 569
- Negative resistance using opamp, 4, 19, 24, 53, 56, 71, 72, 91, 559, 562, 564, 592, 601
- Nodal voltage simulation, 58, 60, 69–73, 102, 232, 246
- Noise analysis of
  - active-RC filters, 600
  - OTA-C filters, 147–246, 251, 287–288, 383, 533, 559, 561
  - SC filters, 1, 6–8, 73, 95, 254–257, 261, 268–272, 276–278, 287, 298–326, 330, 331, 346–349, 351–354, 361–365, 378–381, 424, 426, 439, 578–583
- N-path filters, 306–325, 334
  - double-sampling type, 8, 322–325, 366
- O**
- Offset and gain compensation in SC filters, 8, 337–343, 346
- Operational simulation
  - band-pass filters, 99–100, 291–296, 307, 316, 324, 327, 330, 567–568
  - of general parameter ladder filters, 104–106
  - high-pass filters, 91, 206
  - low-pass elliptic filters, 95
  - using Yoshihoro technique, 102, 105
- Operational simulation based active RC
  - bandpass filters, 283, 293, 302, 321, 420, 461, 539, 601
  - high-pass filters, 100–104, 296–298
  - low-pass elliptic filters, 95
  - low-pass filters, 27–29, 199, 210, 215, 327, 328, 330, 445, 452, 485, 502, 515
- Oscillators, 10, 227–231, 235, 245
  - OTA-C, 3, 8, 147–246, 251, 287–288, 383, 533, 559
- OTA-C filters
  - current-mode filters, 10, 152, 209–212
  - differentiator, 76, 77, 80, 150, 151, 235, 236, 258, 260
  - first-order filters, 27–29, 152–154
  - high-order filters based on component simulation, 197–216
  - integrators, 148–149
  - simulation of Ladder filters, 291–296, 485
  - table based substitution, 202
  - tuning of, 6, 61, 446, 450, 482, 514, 533, 559, 603
  - two-integrator loop OTA-C filters, 63, 81, 82, 100, 154, 155, 164, 168, 169, 172, 175, 184, 236, 262, 329, 378, 379, 402, 477, 493, 519, 533
  - voltage-mode filters, 134
- OTA non-idealities, 206, 223–227
  - pole-zero model, 127, 147, 596
- P**
- Parasitic compensated SC biquad, 268–270
- Passive compensation, 6, 15, 16, 26, 34, 227
- Power dissipation of SC filters, 350, 404–405
- Precision opamp gain technique, 6, 304–306
- Pseudo-N-path filters
  - based on circulating delay line, 311–313
  - based on RAM, 312–316
  - hybrid type, 314, 315
- P*-transformation, 424, 428
- R**
- Realization of R, L, C using SC, 288–291, 296, 316
- Reset-opamp technique, 359–361
- Resistor simulation using OTA, 197–201
  - grounded and floating, 523
- S**
- Sallen–Key filter
  - effect of finite bandwidth, 33–35
  - effect of finite gain, 32–33
- SC
  - amplifiers, 258, 342–346
  - bilinear, 283, 316, 317
  - biquads, 262–270, 272–287, 379, 428
  - capacitor spread evaluation, 265–267
  - delay, 335, 338, 416, 418

SC (*cont.*)

- integrators, 252, 255, 256, 261, 278, 303, 305, 306, 325, 330, 331, 337–346, 349, 351, 352, 354, 359, 360, 366, 368, 375, 377, 379, 404, 405, 408, 424, 426, 583, 584
- LDI type, 257, 289–291, 326, 429
- N-path filters, 306–325
- resistor, 292
- sensitivity of, 265, 267
- Scaling for optimal dynamic range, 67–68, 104
- SCF. *See* Shifted companion form (SCF)
- SC filters
  - distortion in, 346–349
  - effect of finite gain, 409, 410
  - effect of opamp bandwidth, 374–381
  - effect of OTA bandwidth, 350, 378–381
  - offset and gain compensation, 8
  - using comparators, 578–583
- Sensitivity analysis of
  - active RC filters, 5, 88
  - SC filters
- Shifted companion form (SCF), 107, 109–110
- Sigma delta modulators
  - cascaded sigma-delta modulators, 391
    - fourth-order, 391, 392, 396–398, 416, 420, 422
    - high-order, 386, 389–403
  - comparator hysteresis, 411
  - continuous-time, 383
  - effect of bandwidth and slew rate, 407–408, 413
  - effect of capacitor mismatch, 410, 427
  - effect of finite gain, 409, 410
  - effect of jitter, 403–404
  - effect of noise, 405–407

- multi-rate cascaded modulators, 588, 589
- resonator based sigma delta modulator, 415–419, 420–421
- second order, 385–390, 392, 398, 411, 588
  - multistage noise shaping, 389
  - reduced integrator swing range topology, 392
  - using inverters, 584, 589
- Single-path frequency translation, 308–310
- Slew-limited error, 347, 348
- Split-integrating capacitor's T-cell integrator, 273–276, 278–279
- Switch bootstrapping, 350, 355–359
- Switched-opamp technique, 351–354

**T**

- Table-based substitution of OTA-C filters, 202
- Tarmy–Ghausi–Moschytz biquad, 74–76
- Terminations in SC ladder filters, 288
- Tow–Thomas biquad, 62–69, 95, 100, 103, 127, 129, 134, 445, 506, 602
  - variants of Tow–Thomas biquad, 68–74
- Tuning of  $G_m$ -C filters, 447
- Two-amplifier active RC biquads, 132

**U**

- Universal filters, OTA-C, 170, 171
  - derived from digital filters, 195
  - derived from Tarmy–Ghausi configuration, 189–195

**Z**

- $Z$ - $z^N$  transformation, 311, 317, 319, 320, 429